ACS APPLIED MATERIALS & INTERFACES

Research Article

www.acsami.org

# All-Solid-State Lithium Secondary Batteries Using NiS-Carbon Fiber Composite Electrodes Coated with $Li_2S-P_2S_5$ Solid Electrolytes by Pulsed Laser Deposition

Keigo Aso, Atsushi Sakuda, Akitoshi Hayashi, and Masahiro Tatsumisago*

Department of Applied Chemistry, Graduate School of Engineering, Osaka Prefecture University, 1-1 Gakuen-cho, Naka-ku, Sakai, Osaka 599-8531, Japan

**ABSTRACT:** Composite materials including NiS active materials, sulfide-based solid electrolytes (SE), and conductive additives (VGCF: vapor grown carbon fiber) were prepared by coating a highly conductive $Li_2S-P_2S_5$ solid electrolyte onto NiS-VGCF composite using pulsed laser deposition (PLD). From scanning electron microscopy, NiS nanoparticles were on VGCF surface after coating of solid electrolytes using PLD. All-solid-state cells using the SE-coated NiS-VGCF composite and the uncoated NiS-VGCF composite were fabricated, and then the coating effects on the electrochemical performance by forming the SE thin film onto the NiS-VGCF composite were investigated. At a high current density of 3.8 mA $cm^{-2}$ (corresponding to ca. 1 C), an all-solid-state cell fabricated using the SE-coated NiS-VGCF composite as a working electrode showed the initial discharge capacity of 300 mA h $g^{-1}$, and exhibited better cycle performance than the cell using the uncoated NiS-VGCF composite.

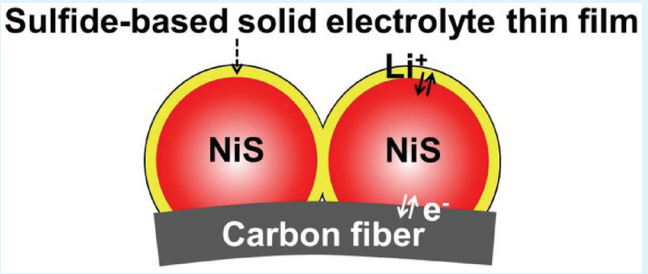


**KEYWORDS:** *all-solid-state battery, lithium secondary battery, NiS-carbon fiber composite, pulsed laser deposition, thin film*

## INTRODUCTION

Lithium-ion batteries are used as power sources for a wide range of portable devices because of their high operating voltage, high energy density, light weight, and longer cycle life.[1] Large-sized lithium-ion batteries with safe characteristics are presently in demand for application as power sources for plug-in hybrid and electric vehicles. All-solid-state lithium secondary batteries that employ inorganic solid electrolytes have attracted much attention, because these batteries are extremely safe, reliable, and free from electrolyte leakage.[2] Much effort has been directed to develop the solid electrolytes with high lithium-ion conductivity. Among many kinds of solid electrolyte, sulfide-based solid electrolytes are promising because of high lithium-ion conductivities at room temperature. Sulfide glasses in the systems $Li_2S$-$SiS_2$ and $Li_2S-P_2S_5$ prepared by the melt-quenching method are known as lithium ion conductors with high conductivities over $10^{-4}$ S $cm^{-1}$ at room temperature.[3−6] Kanno et al. have found that the sulfide crystalline lithium superionic conductor, thio-LISICON (such as solid solutions in the system $Li_4GeS_4-Li_3PS_4$), exhibited high lithium-ion conductivities of $10^{-7}$ to $10^{-3}$ S $cm^{-1}$ at room temperature.[7] Recently, they reported the preparation of $Li_{10}GeP_2S_{12}$ solid electrolyte, which exhibited a quite high lithium-ion conductivity of over $10^{-2}$ S $cm^{-1}$ at room temperature.[8] On the other hand, we have reported that the crystallization of $Li_2S-P_2S_5$ glasses prepared by a mechanical milling technique improved their conductivities.[9] $Li_2S-P_2S_5$ glass-ceramic electrolytes with high lithium-ion conductivity of $5 \times 10^{-3}$ S $cm^{-1}$ at room temperature. In addition, active materials with high capacity and high rate capability have been investigated for development of all-solid-state batteries.[10]

In bulk-type all-solid-state batteries, an electrode is a mixture of three constituents of active materials, solid electrolytes (lithium ion conduction path), and conductive additives (electron conduction path). Electrochemical reactions proceed at the solid−solid interface and are affected by the states of the interface in the electrode. It is expected that the solid−solid interface in the electrode will increase with decreasing the particle size of monodispersed active materials. We reported that monodispersed $\alpha$-$Fe_2O_3$ particles of various sizes were synthesized by a solution process using a NaOH aqueous solution.[11] The all-solid-state cell with a submicrometer $\alpha$-$Fe_2O_3$ electrode exhibited higher capacity than that of the cell using a micrometer-size $\alpha$-$Fe_2O_3$ electrode. In addition, we reported that NiS nanoparticles with the size of 50 nm were synthesized in high-boiling solvents.[12] The all-solid-state cells using the obtained NiS nanoparticles exhibited a large capacity of 680 mA h $g^{-1}$ after 20 cycles at 0.13 mA $cm^{-2}$. Charge−discharge potential of the all-solid-state cells using NiS as an active material was low, and the average potential of the cell was about 1.5 V (vs Li). Several articles reported that NiS was used as a positive electrode in electrochemical cells using a liquid electrolyte.[13−15] On the other hand, NiS is useful as a negative

Received: September 30, 2012
Accepted: January 15, 2013
Published: January 15, 2013

  

electrode with the combination of 5 V class positive electrode materials, which can be applied to all-solid-state batteries.

Nanomaterials prepared by a solution process using high-boiling solvents have been attracting attention.[16] It was reported that various metal phosphides such as MnP, $Co_2P$, FeP, and $Ni_2P$, and sulfides such as $Cu_2S$, ZnS, MnS, and PbS were synthesized using this process,[17,18] which is a facile route to synthesize nanoparticles having uniform size with various morphologies. We reported that phase-controlled and morphology-controlled active materials (NiS and SnS) synthesized by this process were applied to all-solid-state cells.[12,19] The all-solid-state cells exhibited a large capacity of 600−1000 mA h $g^{-1}$ and excellent cycle performance. Nanocomposites, in which nanosized active materials with less suppression of aggregation have contacts with solid electrolytes and conductive additives, are preferable as electrodes for use in all-solid-state batteries to form favorable lithium ion and electron conduction paths.

To improve rate capability of all-solid-state batteries, increased contact area among active material, solid electrolyte, and conductive additive in a composite working electrode is necessary. Several papers about the preparation of composite working electrodes have been reported.[20−22] We reported that NiS-VGCF (VGCF: vapor grown carbon fiber) composites were synthesized using high-boiling solvents as reaction media in order to form favorable electron conduction paths for NiS active materials, and that the electrochemical performance of the all-solid-state cells was affected by the particle aggregation of NiS active materials in the working electrode;[23] an all-solid-state cell fabricated using the mixture of the NiS-VGCF composite and sulfide-based solid electrolyte (SE) particles as a working electrode showed the initial discharge capacity of 590 mA h $g^{-1}$ at 1.3 mA $cm^{-2}$, and exhibited better cycle performance than the cell using the mixture of NiS, VGCF, and SE particles. In addition, we reported that a highly conductive $Li_2S-P_2S_5$ SE was coated on $LiCoO_2$ particles using pulsed laser deposition (PLD) to form intimate solid−solid contacts between $LiCoO_2$ and SE.[24]

Figure 1 shows the schematic illustration of our proposal composite electrode. We believe that the use of carbon fiber forms a continuous electron conducting paths in the composite electrode, and active material with uniform size contacts intimately with both carbon fiber and solid electrolyte. In this study, NiS-VGCF-SE composite were first prepared by coating the $80Li_2S{\cdot}20P_2S_5$ (mol %) SE onto the NiS-VGCF composite using PLD to form favorable lithium ion and electron conduction paths for the NiS active material (Figure 1), and we will discuss the importance of formation of lithium-ion conduction paths in the working electrode for all-solid-state cells. All-solid-state cells using the SE-coated NiS-VGCF composite and using uncoated NiS-VGCF composite were fabricated. Electrochemical properties of the cells were investigated using charge−discharge measurements.

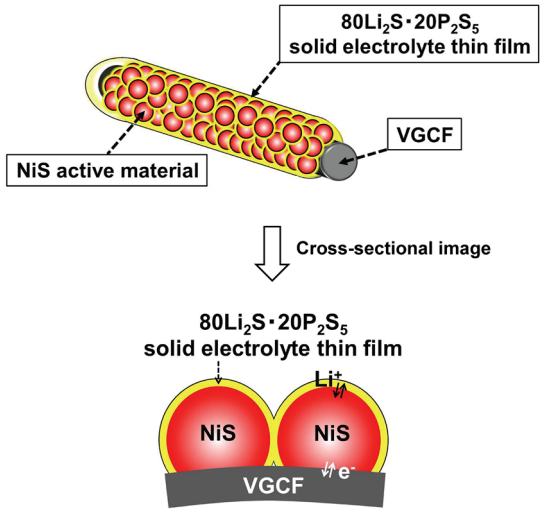


**Figure 1.** Schematic illustration of the SE-coated NiS-VGCF composite. SE denotes the $80Li_2S{\cdot}20P_2S_5$ (mol %) solid electrolyte.

## EXPERIMENTAL SECTION

In our previous paper, NiS-VGCF composites were synthesized using thermal decomposition of nickel acetylacetonate and 1-dodecanethiol as a sulfur source in a mixture of VGCF and 1-octadecene as a solvent.[23] The mixture was heated in a flask to 280 °C and was subsequently kept at 280 °C for 5 h under stirring in an Ar atmosphere. An $80Li_2S{\cdot}20P_2S_5$ (mol %) solid electrolyte (SE) was coated on the NiS-VGCF composites using pulsed laser deposition (PLD). SE thin films of $80Li_2S{\cdot}20P_2S_5$ were fabricated using PLD with a KrF excimer laser ($\lambda$ = 248 nm, LPXPro, Lambda Physik).[25] A pelletized mixture of $Li_2S$ and $P_2S_5$ powder with a molar ratio of 80:20 was used as a target. The $80Li_2S{\cdot}20P_2S_5$ films deposited on Si substrates were amorphous and showed the lithium ion conductivity of $7.9 \times 10^{-5}$ S $cm^{-1}$ at 25 °C.[25] Target holders were attached to the upper side of a PLD vacuum chamber, and a vibrating sample holder was equipped at the lower side. This PLD system allowed the formation of an SE layer on the electrode particles. During deposition of the SE, the NiS-VGCF composite powders were fluidized by a vibration system (VIB-FB, Nara Machinery Co., Ltd.) to form a uniform SE layer on the NiS-VGCF composites. The frequency of the square pulse used to fluidize the particles was 500 Hz and the deposition time was 120 min. The morphology of the obtained SE-coated NiS-VGCF composites was investigated using scanning electron microscopy (SEM; JSM-6610A; JEOL) coupled with an energy dispersive X-ray spectrometer (EDX; JED-2300; JEOL) and transmission electron microscopy (TEM; JEM-2100F; JEOL).

Laboratory-scale solid-state cells were fabricated as follows. The $80Li_2S{\cdot}20P_2S_5$ (mol %) glass-ceramic solid electrolyte powder was prepared by mechanical milling of a mixture of $Li_2S$ and $P_2S_5$ and subsequent heat treatment. The prepared electrolyte exhibited a wide electrochemical window and high ionic conductivity at room temperature.[9] The working electrodes which consisted of the SE-coated NiS-VGCF composite (100, 80, and 40 wt %) and the glass-ceramic electrolyte (0, 20, and 60 wt.%) were prepared by hand-grinding of the mixtures in a mortar. For comparison, a working electrode which consisted of the uncoated NiS-VGCF composite (40 wt.%) and the glass-ceramic electrolyte (60 wt.%) were prepared by hand-grinding of the mixture in a mortar. Two-electrode cells were fabricated using a working electrode, the glass-ceramic electrolyte, and a Li−In alloy as a counter electrode. The working electrode and solid electrolyte were placed in a polycarbonate tube (10 mm diameter) and pressed together under 360 MPa at room temperature. The Li−In alloy was placed on the surface of the solid electrolyte side of the bilayer pellet. Then pressure of 120 MPa was applied to obtain a three-layered pellet. The three-layered pellet was finally sandwiched with two stainless-steel disks as current collectors. All preparation processes of the cells were conducted in a dry Ar-filled glovebox. Electrochemical tests were conducted under a constant current density of 1.3 and 3.8 mA $cm^{-2}$ at 25 °C in an Ar atmosphere using a charge−discharge measurement device (BTS-2004, Nagano Co.).

## RESULTS AND DISCUSSION

Figure 2a, b show the SEM image and EDX mapping for Ni element of the NiS-VGCF composite coated with the


dx.doi.org/10.1021/am302164e | ACS Appl. Mater. Interfaces 2013, 5, 686−690

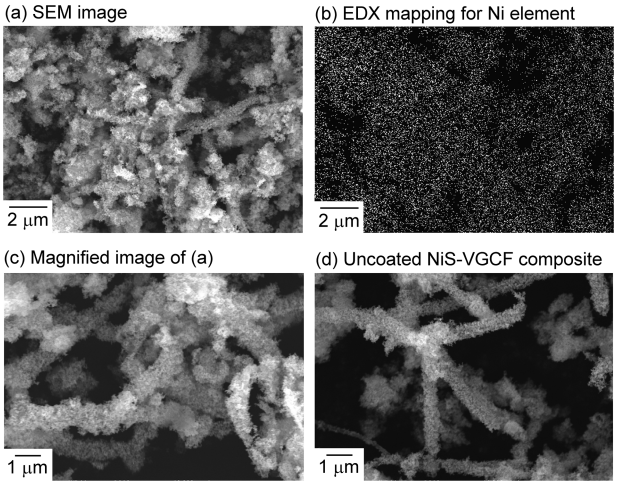


**Figure 2.** (a) SEM image and (b) EDX mapping for nickel element of the SE-coated NiS-VGCF composite. (c) Magnified image of a. (d) SEM image of the uncoated NiS-VGCF composite.

$80Li_2S{\cdot}20P_2S_5$ (mol %) solid electrolyte (SE) by pulsed laser deposition (PLD). The signals of EDX mapping for Ni element were uniformly distributed in Figure 2b. Figure 2c is a magnified image of Figure 2a. Figure 2d shows the SEM image of the uncoated NiS-VGCF composite for comparison. In our previous paper, NiS nanoparticles with the size of 50 nm were formed on VGCF surface in the uncoated NiS-VGCF composites.[23] NiS nanoparticles were on VGCF surface after SE-coating by using PLD, and morphology of the SE-coated NiS-VGCF composite was not largely changed from the uncoated NiS-VGCF composite. Images a and b in Figure 3

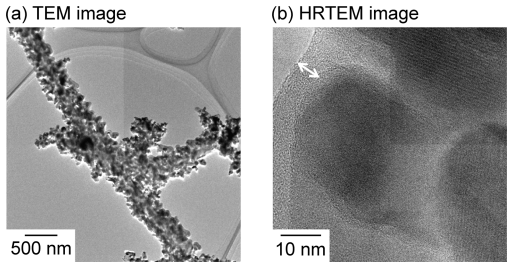


**Figure 3.** (a) TEM and (b) HRTEM images of the SE-coated NiS-VGCF composite. An amorphous SE thin film was denoted with an arrow in b.

show the TEM and high-resolution TEM (HRTEM) images of the SE-coated NiS-VGCF composite. In Figure 3b, an amorphous SE thin film with the thickness of ca. 5 nm was observed on NiS nanoparticles with lattice fringes (the amorphous SE thin film was denoted with an arrow).

Panels a and b in Figures 4 respectively show the charge–discharge curves of the all-solid-state cells with the working electrodes using 100 wt % SE-coated NiS-VGCF composites and those using a mixture of 80 wt % SE-coated NiS-VGCF composites and 20 wt % solid electrolyte (SE) particles, at a current density of 0.64 mA $cm^{-2}$. Li–In alloy was used as a counter electrode because Li–In alloy exhibits a stable potential plateau at 0.62 V vs $Li^+$/Li, as observed in all-solid-state cells with sulfide electrolytes. In panels a and b in Figure 4, the left-side ordinate axis shows the electrode potential vs Li–In, while the right-side ordinate axis shows the electrode potential vs Li, which is calculated based on the potential difference between

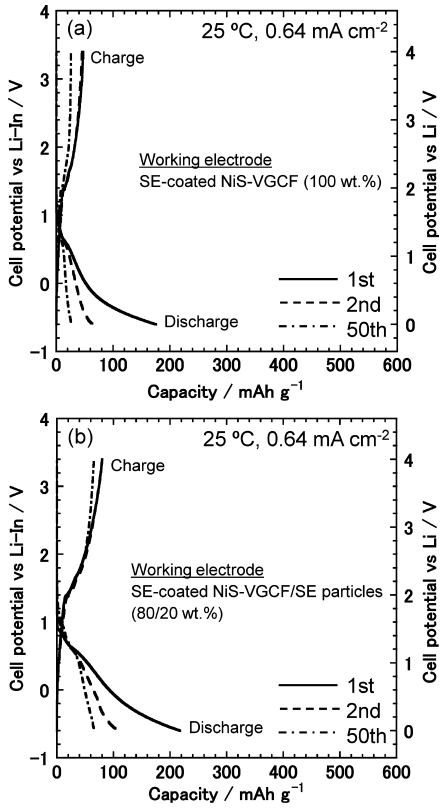


**Figure 4.** Charge–discharge curves of the all-solid-state cells with the working electrodes using (a) 100 wt % SE-coated NiS-VGCF composites, or (b) a mixture of 80 wt % SE-coated NiS-VGCF composites and 20 wt % solid electrolyte (SE) particles, at a current density of 0.64 mA $cm^{-2}$.

Li–In and Li electrodes (0.62 V). In order to evaluate the electrochemical performance of the cells using the newly designed working electrode, the discharge measurements were performed up to 0 V (vs Li) in this study. The obtained capacity was normalized according to the weight of the SE-coated NiS-VGCF composite in the working electrode. The initial charge–discharge capacity and efficiency of the cell with the working electrode using 100 wt % SE-coated NiS-VGCF composite was low; the initial discharge capacity (175 mA h $g^{-1}$) of the cell with the working electrode using 100 wt % SE-coated NiS-VGCF composite was lower during 50 cycles than the initial capacity (220 mA h $g^{-1}$) of the cell with the working electrode using a mixture of 80 wt % SE-coated NiS-VGCF composites and 20 wt.% SE particles. This result suggests that the formation of lithium-ion conduction paths is not sufficient in the working electrode with 100 wt % SE-coated NiS-VGCF composites, and the addition of SE particles is effective for the formation of lithium-ion conduction paths. Figure 5 shows the charge–discharge curves of the all-solid-state cell with the working electrode using a mixture of 40 wt % SE-coated NiS-VGCF composites and 60 wt % SE particles under the current density of 1.3 mA $cm^{-2}$. Even at a higher current density of 1.3 mA $cm^{-2}$, the cell exhibited the charge–discharge efficiency of approximately 100% and a large capacity of 430 mA h $g^{-1}$ at the 50th cycle. This is because the addition of SE particles gives the favorable lithium ion conduction paths in the working electrode.

Panels a and b in Figure 6 show the charge–discharge curves all-solid-state cell using the uncoated or SE-coated NiS-VGCF


dx.doi.org/10.1021/am302164e | ACS Appl. Mater. Interfaces 2013, 5, 686–690

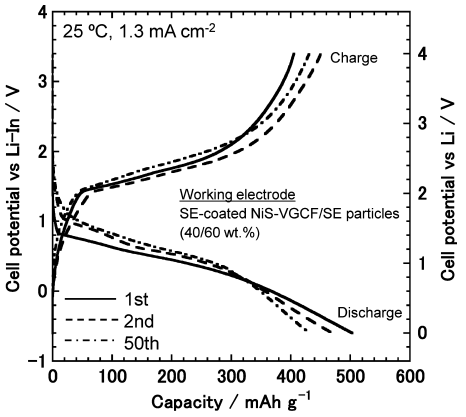


**Figure 5.** Charge−discharge curves of the all-solid-state cell with the working electrode using a mixture of 40 wt % SE-coated NiS-VGCF composites and 60 wt % SE particles at a current density of 1.3 mA $cm^{-2}$.

composite at the first, second, and 50th cycles under the current density of 3.8 mA $cm^{-2}$ (corresponding to ca. 1 *C*). The two working electrodes consisted of the 40 wt % uncoated or SE-coated NiS-VGCF composites, and 60 wt % SE particles. The obtained capacity of the cell using the uncoated or SE-coated NiS-VGCF composite was normalized according to the total weight of the uncoated or SE-coated NiS-VGCF composite in the working electrode. At the first cycle, the charge−discharge efficiency of the cell with the SE-coated NiS-VGCF composite is higher than that of the cell with the uncoated NiS-VGCF composite. As a result, the discharge capacity (240 mA h $g^{-1}$) of the cell with the SE-coated NiS-VGCF composite is larger at the second cycle than the capacity (100 mA h $g^{-1}$) of the cell with the uncoated NiS-VGCF composite. Figure 6c shows the cycle performance of all-solid-state cells using the uncoated or SE-coated NiS-VGCF composite at the current density of 3.8 mA $cm^{-2}$. At a high current density of 3.8 mA $cm^{-2}$, an all-solid-state cell fabricated using the SE-coated NiS-VGCF composite as a working electrode showed the initial discharge capacity of 300 mA h $g^{-1}$, and exhibited better cycle performance than the cell using the uncoated NiS-VGCF composite. This result suggests that the formation of intimate interfaces among NiS, VGCF, and SE gives favorable electron and lithium ion conduction paths to NiS nanoparticles (see Figure 1). At the present stage, the formation of lithium-ion conduction paths was not sufficient in the working electrode with 100 wt % SE-coated NiS-VGCF composites, and the addition of SE particles in the working electrode was necessary to fabricate the all-solid-state cells with high capacity. However, the use of the SE-coated NiS-VGCF composite was more effective in improving the electrochemical performance at a high current density of 3.8 mA $cm^{-2}$ (ca. 1 *C*) than that of the uncoated NiS-VGCF composite.

## ■ CONCLUSIONS

Composite materials with NiS active materials, solid electrolytes (SE), and conductive additives (VGCF: vapor grown carbon fiber) were prepared by coating $Li_2S-P_2S_5$ SE onto the NiS-VGCF composite using pulsed laser deposition (PLD) to form favorable lithium ion and electron conduction paths for the NiS active materials. NiS nanoparticles were on the VGCF

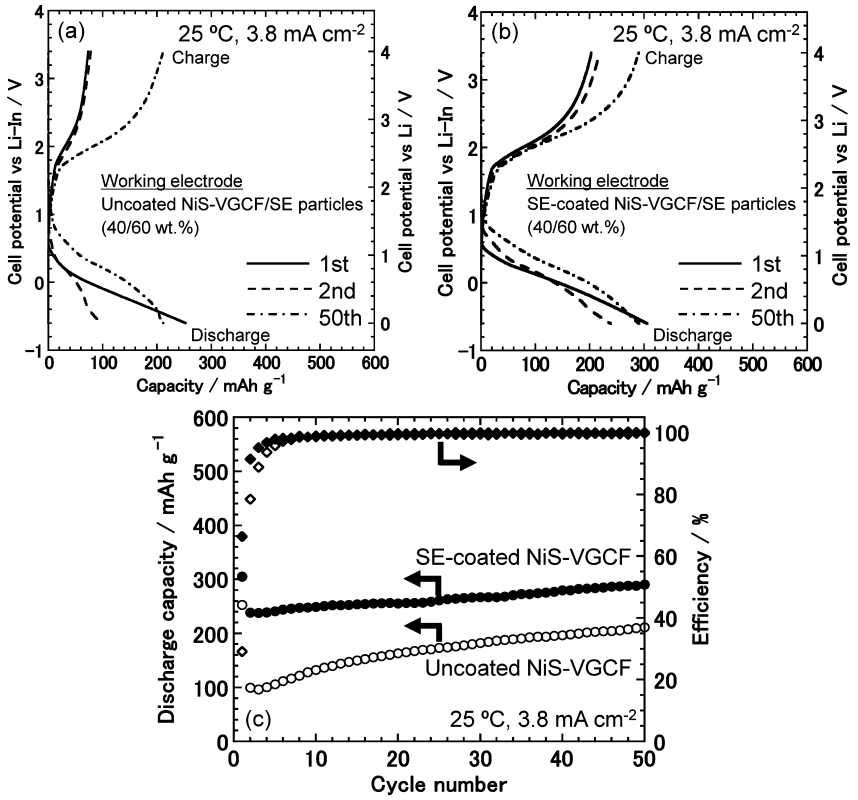


**Figure 6.** Charge−discharge curves of all-solid-state cell using (a) uncoated or (b) SE-coated NiS-VGCF composite at the first, second, and 50th cycles under the current density of 3.8 mA $cm^{-2}$. (c) Cycle performance of all-solid-state cell using the uncoated or SE-coated NiS-VGCF composite at the current density of 3.8 mA $cm^{-2}$ (corresponding to ca. 1 *C*).


dx.doi.org/10.1021/am302164e | *ACS Appl. Mater. Interfaces* 2013, 5, 686−690

surface after the deposition of SE thin films. At a high current density of 3.8 mA $cm^{-2}$ (ca. 1 *C*), an all-solid-state cell fabricated using the SE-coated NiS-VGCF composite as a working electrode showed the initial discharge capacity of 300 mAh $g^{-1}$, and exhibited better cycle performance than the cell using uncoated the NiS-VGCF composite. Electrochemical performance in all-solid-state cells was improved by forming favorable NiS-VGCF-SE interfaces.

## AUTHOR INFORMATION


### Corresponding Author

*Tel.: +81-72-2549331. Fax.: +81-72-2549331. E-mail: tatsu@chem.osakafu-u.ac.jp.


### Notes

The authors declare no competing financial interest.

## ACKNOWLEDGMENTS

This research was financially supported by the Japan Science and Technology Agency (JST), Core Research for Evolutional Science and Technology (CREST) project. K.A. is thankful for a Grant-in-Aid received as a Japan Society for the Promotion of Science (JSPS) Fellow. We thank Professor Shigeo Mori at Osaka Prefecture University for high-resolution TEM observation of the SE-coated NiS-VGCF composite.

## REFERENCES


(1) Tarascon, J. M.; Armand, M. *Nature* **2001**, *414*, 359−367.
(2) Fergus, J. W. *J. Power Sources* **2010**, *195*, 4554−4569.
(3) Mercier, R.; Malugani, J.-P.; Fahys, B.; Robert, G. *Solid State Ionics* **1981**, *5*, 663−666.
(4) Pradel, A.; Ribes, M. *Solid State Ionics* **1986**, *18/19*, 351−355.
(5) Kennedy, J. H. *Mater. Chem. Phys.* **1989**, *23*, 29−50.
(6) Minami, T.; Hayashi, A.; Tatsumisago, M. *Solid State Ionics* **2000**, *136−137*, 1015−1023.
(7) Kanno, R.; Murayama, M. *J. Electrochem. Soc.* **2001**, *148*, A742−A746.
(8) Kamaya, N.; Homma, K.; Yamakawa, Y.; Hirayama, M.; Kanno, R.; Yonemura, M.; Kamiyama, T.; Kato, Y.; Hama, S.; Kawamoto, K.; Mitsui, A. *Nat. Mater.* **2011**, *10*, 682−686.
(9) Mizuno, F.; Hayashi, A.; Tadanaga, K.; Tatsumisago, M. *Adv. Mater.* **2005**, *17*, 918−921.
(10) Nagao, M.; Kitaura, H.; Hayashi, A.; Tatsumisago, M. *J. Power Sources* **2009**, *189*, 672−675.
(11) Kitaura, H.; Takahashi, K.; Mizuno, F.; Hayashi, A.; Tadanaga, K.; Tatsumisago, M. *J. Electrochem. Soc.* **2007**, *154*, A725−A729.
(12) Aso, K.; Kitaura, H.; Hayashi, A.; Tatsumisago, M. *J. Mater. Chem.* **2011**, *21*, 2987−2990.
(13) Han, S.-C.; Kim, H.-S.; Song, M.-S.; Lee, P. S.; Lee, J.-Y.; Ahn, H.-J. *J. Alloy. Compd.* **2003**, *349*, 290−296.
(14) Wang, J.-Z.; Chou, S.-L.; Chew, S.-Y.; Sun, J.-Z.; Forsyth, M.; MacFarlane, D. R.; Liu, H.-K. *Solid State Ionics* **2008**, *179*, 2379−2382.
(15) Takeuchi, T.; Sakaebe, H.; Kageyama, H.; Handa, K.; Sakai, T.; Tatsumi, K. *J. Electrochem. Soc.* **2009**, *156*, A958−A966.
(16) Park, J.; Joo, J.; Soon, G. K.; Jang, Y.; Hyeon, T. *Angew. Chem., Int. Ed.* **2007**, *46*, 4630−4660.
(17) Park, J.; Koo, B.; Yoon, K. Y.; Hwang, Y.; Kang, M.; Park, J.-G.; Hyeon, T. *J. Am. Chem. Soc.* **2005**, *127*, 8433−8440.
(18) Choi, S.-H.; An, K.; Kim, E.-G.; Yu, J. H.; Kim, J. H.; Hyeon, T. *Adv. Funct. Mater.* **2009**, *19*, 1645−1649.
(19) Aso, K.; Hayashi, A.; Tatsumisago, M. *Cryst. Growth Des.* **2011**, *11*, 3900−3904.
(20) Nagao, M.; H.; Hayashi, A.; Tatsumisago, M. *J. Mater. Chem.* **2012**, *22*, 10015−10020.
(21) Trevey, J. E.; Stoldt, C. R.; Lee, S. H. *J. Electrochem. Soc.* **2011**, *158*, A1282−A1289.
(22) Nagao, M.; Imade, Y.; Narisawa, H.; Kobayashi, T.; Watanabe, R.; Yokoi, T.; Tatsumi, T.; Kanno, R. *J. Power Sources* **2013**, *222*, 237−242.
(23) Aso, K.; Hayashi, A.; Tatsumisago, M. *Electrochim. Acta* **2012**, *83*, 448−453.
(24) Sakuda, A.; Hayashi, A.; Ohtomo, T.; Hama, S.; Tatsumisago, M. *J. Power Sources* **2011**, *196*, 6735−6741.
(25) Sakuda, A.; Hayashi, A.; Hama, S.; Tatsumisago, M. *J. Am. Ceram. Soc.* **2010**, *93*, 765−768.